

RSC Advances



This is an *Accepted Manuscript*, which has been through the Royal Society of Chemistry peer review process and has been accepted for publication.

Accepted Manuscripts are published online shortly after acceptance, before technical editing, formatting and proof reading. Using this free service, authors can make their results available to the community, in citable form, before we publish the edited article. This *Accepted Manuscript* will be replaced by the edited, formatted and paginated article as soon as this is available.

You can find more information about *Accepted Manuscripts* in the [Information for Authors](#).

Please note that technical editing may introduce minor changes to the text and/or graphics, which may alter content. The journal's standard [Terms & Conditions](#) and the [Ethical guidelines](#) still apply. In no event shall the Royal Society of Chemistry be held responsible for any errors or omissions in this *Accepted Manuscript* or any consequences arising from the use of any information it contains.

ARTICLE

Optical, electrochemical, third order nonlinear optical, and excited state dynamics studies of *bis*(3,5-trifluoromethyl)phenyl-zinc phthalocyanine

Cite this: DOI: 10.1039/x0xx00000x

Narra Vamsi Krishna,^a Varun Kumar Singh,^a Debasis Swain,^b Soma Venugopal Rao,^{b*} Lingamallu Giribabu^{a*}

Received 00th January 2014,

Accepted 00th January 2014

DOI: 10.1039/x0xx00000x

Zinc phthalocyanine with *bis*(3,5-trifluoromethyl)phenyl groups at peripheral positions has been synthesized and its optical, emission, electrochemical and third-order nonlinear optical properties were investigated. Both the Soret and Q bands were red-shifted and obeyed Beer-Lambert's law. Electrochemical properties indicated that both oxidation and reduction processes were ring centred. Emission spectra were recorded in different solvents and the fluorescence yields obtained were in the range of 0.29 to 0.10 while the time-resolved fluorescence data revealed lifetimes of typically few ns. Nonlinear optical coefficients were retrieved from the Z-scan measurements using picosecond and femtosecond pulses. Excited state lifetime was deduced from the femtosecond degenerate pump-probe measurements. Our data suggests that this compound has potential for applications in the field of photonics.

Introduction

Nonlinear optical (NLO) materials play a pivotal role in the future evolution of photonics in general and its impact in technology and industrial applications in particular.¹⁻³ The goal is to find and develop materials presenting large nonlinearities and satisfying at the same time all the technological requirements for applications such as wide transparency range, ultrafast response, high damage threshold nonetheless processability, adaptability and interfacing with other materials. NLO active materials displaying both second- and third-order NLO properties such as second harmonic generation, third harmonic generation and optical limiting.⁴⁻⁷ Among all the NLO applications, optical limiting is one of the most promising in practice, used in applications such as the protection of human eyes and optical sensors.⁸⁻¹¹ Several mechanisms could lead to optical limiting behaviour, such as reverse saturable absorption, two photon absorption, nonlinear refraction and optically induced scattering.¹²⁻¹⁴ Organic NLO materials continue attracting attention because of their additional potential application in the fields of optical communications, optical storage, optical computing, harmonic generation, optical switching, etc. In the context of NLO active materials, organic dyes with long π -conjugated structures have attracted consideration owing to their interesting electronic and optical characteristics.¹⁵⁻¹⁷

Phthalocyanines type organic dyes with highly conjugated aromatic cycle have thus emerged as exceptional candidates for NLO applications.¹⁸ Phthalocyanine derivatives are thermally, optically, and chemically stable.¹⁹ Moreover, their NLO properties have been actively studied by many researchers in this field including our group.²⁰⁻²⁸ Phthalocyanines are remarkable molecules with a characteristic sharp Q-band arising from the π - π^* absorption in the 600-700 nm region (Q-bands) and a Soret band in the 300-450 nm region. The sharp Q-bands with high molar extinction coefficient in the far visible region is the source of inspiration for such molecules to be able to find applications in the chemical sensors, electrochromic displays, liquid crystals, photodynamic therapy, dye sensitized solar cells and catalysis.²⁹⁻³² What makes phthalocyanines even more susceptible to NLO applications is the choice of modifications in the periphery and the possibility of accommodating more than 70 different elements in the core of the macrocycle directed towards tailoring of these molecules. But what makes drawback in these macrocycles is their lack of solubility in common organic solvents and their tendency to aggregate at higher concentrations. As a result, optimum structural design by use of specific functional groups at the periphery can be synthesized to find particular applications. Recently, we have introduced the sterically hindered phthalocyanine derivatives for applications in non-linear optical applications with strong NLO coefficients possibly because of the long-lived lifetimes.³³ In our efforts towards synthesis of efficient phthalocyanine macrocycle capable of achieving strong NLO responses we have designed *bis*-trifluoromethyl phenyl substituted phthalocyanines. The trifluoromethyl group is strongly electron withdrawing and bulky with a van der Waals radius of 2.2 Å⁰ or more, thus we anticipated that the introduction of trifluoromethyl groups onto the phthalocyanine periphery would impact the electronic and steric properties of the macrocycle. Also fluorine compounds are known to enhance the solubility of phthalocyanine in polar aprotic

^aInorganic and Physical Chemistry Division, Indian Institute of Chemical Technology, Hyderabad 500 007, India

^bAdvanced Centre of Research in High Energy Materials (ACRHEM), University of Hyderabad, Prof. C.R. Rao Road, Hyderabad 500046, Andhra Pradesh, India

*Corresponding author e-mail: giribabu@iict.res.in; svrsp@uohyd.ernet.in

† Electronic Supplementary Information (ESI) available: ESI-MS, IR, ¹H NMR, MALDI-TOF-MS spectra are provided in SI

solvents as well as shifts the redox processes towards positive potentials. Some groups have previously reported phthalocyanines with trifluoromethyl groups.³⁴⁻³⁶ However, no studies of NLO applications are reported so far to the best of our knowledge. We report here a new phthalocyanine molecule conjugated with 3,5-bis(trifluoromethyl)phenyl substituent at the four peripheral positions as shown in Scheme 1. We have studied the aggregation properties, electrochemical, spectro-electrochemical, excited state dynamics and the NLO properties of the new zinc phthalocyanine.

Experimental section

Materials

4-Iodophthalonitrile, bis(3,5-trifluoromethyl)phenylboronic acid, 1-pentanol, 1,8-diazabicyclo[5.4.0] undec-7-ene and bis(triphenylphosphine)palladium(II) dichloride were purchased from sigma Aldrich and were used as such. All the solvents viz., dichloromethane, tetrahydrofuran, dimethylsulfoxide, N,N-dimethylformamide, toluene, chloroform, methanol were purchased from SD Fine chemicals limited, India and were dried before further use. Zinc(II)acetate and sodium carbonate were purchased from Qualigen Chemicals Ltd, India.

Synthesis

Bis(3,5-trifluoromethyl)phenylphthalonitrile (1): A seal tube with a teflon cap was charged with 4-Iodophthalonitrile (0.32 g, 1.26 mmol), 3,5-bis(trifluoromethyl)phenyl boronic acid (1.0 g, 3.88 mmol), catalytic amount of bis(triphenylphosphine)palladium(II) dichloride and then flushed with nitrogen for 15 minutes before the addition of solvent tetrahydrofuran. To this 2M sodium carbonate (aq.) was added and the seal tube was capped in nitrogen atmosphere. The reaction mixture was stirred at 70 °C for 6 h. After cooling to room temperature, the reaction mixture was washed twice with water. The combined organic layers were washed once with water, subsequently dried over anhydrous Na₂SO₄, filtered and concentrated under rotary evaporator. The resultant residue was subjected to silica gel column chromatography and eluted with hexane-ethyl acetate (90/10% v/v) to obtain the desired product as white powder. Elemental analysis of Anal. Calcd. For C₁₆H₆F₆N₂% (340.23): C, 56.48; H, 1.78; N, 8.23. Found: C, 56.45; H, 1.79; N, 8.24. ESI-MS (m/z): C₁₆H₆F₆N₂ [340.23]; M⁺ 343. ¹H NMR (300 MHz, CDCl₃): δ (ppm) 8.05 (m, 1H), 8.02 (s, 3H), 7.98 (d, J_{HH} = 1.22, 2H); FT-IR (KBr) ν_{max} 2238 (CN) cm⁻¹.

TFM-Pc: A mixture of anhydrous zinc acetate (1.90g, 10 mmol), Bis(3,5-trifluoromethyl)phenylphthalonitrile (**1**) (1.70 g, 5 mmol), DBU (catalytic amount) and dry 1-pentanol (5 ml) was refluxed at 150°C for 16 h under nitrogen atmosphere. After cooling, the solution was precipitated by methanol, filtered and dried. The obtained solid materials was subjected to silica gel column chromatography and eluted with dichloromethane. The green coloured band was collected and recrystallized from methanol, to get the desired compound 70% yield. Elemental analysis of Anal. Calcd. For C₆₄H₂₄F₂₄N₈Zn% (1426.29): C, 53.90; H, 1.70; N, 7.86. Found: C, 53.81; H, 1.74; N, 7.85. MALDI-TOF (m/z): C₆₄H₂₄F₂₄N₈Zn [1426.29]: 1426.15 (M⁺), FT-IR (KBr) ν_{max} 2928, 2840, 1254 and 1024 cm⁻¹. UV-Vis: (in DCM, λ_{max}, ε M⁻¹cm⁻¹) 682 (99,800), 616 (27,000), 349 (51,400).

Instrumentation

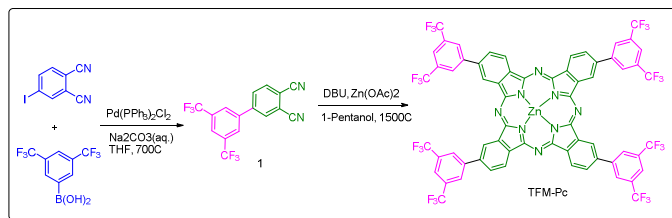
Absorption spectra were recorded with a Shimadzu UV-3600, UV-Visible-NIR spectrophotometer. Steady-state fluorescence spectra were recorded using a Fluorolog-3 spectrofluorometer (Spex model, JobinYvon) for solutions with optical density at the wavelength of excitation (λ_{ex}) ≈ 0.05. Fluorescence quantum yields (φ) were estimated by integrating the fluorescence bands zinc *tert*-butyl phthalocyanine (φ=0.37 in benzene).³⁷ Fluorescence lifetime measurements were carried on a picosecond time-correlated single photon counting (TCSPC) setup (FluoroLog3-Triple Illuminator, IBH Horiba JobinYvon) employing a picosecond light emitting diode laser (NanoLED, λ_{ex} = 670 nm) as excitation source. The decay curves were recorded by monitoring the fluorescence emission maxima of the phthalocyanine macrocycle (λ_{em} = 700 nm). Photomultiplier tube (R928P, Hamamatsu) was employed as the detector. The lamp profile was recorded by placing a scattered (dilute solution of Ludox in water) in place of the sample. The width of the instrument function was limited by the full width at half maximum (FWHM) of the excitation source, ~635 ps at 670 nm. Decay curves were analyzed by nonlinear least-squares iteration procedure using IBH DAS6 (version 2.3) decay analysis software. The quality of the fits was judged by the χ² values and distribution of the residuals.

Electrochemical measurements were performed on a PC-controlled CH instruments model CHI 620C electrochemical analyzer. The experiments were performed on 1 mM phthalocyanine solution in CH₂Cl₂ solvent at scan rate of 100 mV/s using 0.1 M tetrabutyl ammonium perchlorate (TBAP) as supporting electrolyte. The working electrode was glassy carbon, standard calomel electrode (SCE) was reference electrode and platinum wire was an auxiliary electrode. After a cyclic voltammogram (CV) had been recorded, ferrocene was added, and a second voltammogram was measured. The optical thin layer electrochemical studies were carried on Maya 2000 Ocean Optics software using DT-MINI-2-GS, UV-VIS-NIR LIGHTSOURCE. ¹H NMR spectra were recorded in CDCl₃ solutions on AVANCE 300 MHz spectrophotometer using TMS as standard. FT-IR spectra (KBr pellets) were recorded on a Perkin Elmer Spectrophotometer. Mass spectra were acquired using ElectroSpray Ionization (ESI) method, operated in positive ion mode using m/z range 100-2000 and MALDI-TOF analysis.

NLO and pump-probe studies

The Z-scan³⁸⁻⁴¹ measurements were performed using ~2 picosecond (ps) pulses at 800 nm and ~70 femtosecond (fs) pulses at 690 nm. The ps/fs experiments were performed on solutions (samples dissolved in THF) with typically 0.7 mM concentration. In the fs case beam waist at focus was estimated to be ~22 μm with a corresponding Rayleigh range of 2.2 mm. In the ps case beam waist at focus was estimated to be ~35 μm with a corresponding Rayleigh range of 4.5 mm. The degenerate pump-probe experiments were performed at 600 nm using ~70 fs pulses from an optical parametric amplifier which was pumped by ~40 fs pulses from an amplifier (Coherent). Pump-probe power ratios were typically 40-50. The probe diameter was <1 mm. The probe was aligned such that it always within the pump diameter of ~3 mm. Data was acquired

through the combination of a photo-diode and lock-in amplifier. Complete details can be found in some of our earlier works.³⁸⁻⁴¹



Scheme 1: Synthetic route of TFM-Pc.

Results and Discussion

The synthetic route to new phthalocyanine **TFM-Pc** is shown in **Scheme 1**. This complex was prepared by the template cyclotetramerization of *Bis*(3,5-trifluoromethyl)phenylphthalonitrile (**1**) with anhydrous zinc acetate in 1-pentanol at reflux temperature under nitrogen atmosphere in the presence of DBU as a non-nucleophilic base catalyst. The phthalocyanine was purified by silica gel column chromatography and characterized by elemental analysis, Mass, FT-IR, ¹H-NMR, UV-Vis., and emission spectroscopy as well as electrochemical techniques. The elemental analysis of **TFM-Pc** as shown in experimental section was found to be satisfactory. The MALDI-TOF mass spectrum of phthalocyanine consists of molecular ion peak at m/z 1426.15 (M^+), which confirms the presence of phthalocyanine macrocycle (See supporting information). The absence of '-CN' stretching group in the FT-IR spectrum of phthalocyanine further supports the macrocycle formation.

UV-Visible absorption studies

Typical UV-Visible absorption spectra of monomeric phthalocyanines show two featured absorption bands, namely the Q-band and B-band, which can be readily interpreted by using Gouterman's four orbital model.⁴² These intense band systems can be shifted or broadened depending upon peripheral substitution, metallation and aggregation of the molecules. The electronic absorption spectra of phthalocyanine in various solvents in the concentration range $1.0 \times 10^{-5} \text{ M}^{-1} \text{ cm}^{-1}$ are shown in Figure 1. At this concentration the absorption spectrum of the phthalocyanine molecule looks same for all solvents except DCM and toluene where an increase in the absorption above 700 nm was noticed. This difference in the absorption above 700 nm is anticipated to be due to the J-aggregation. As the solvents THF, DMF and DMSO are coordinating solvents therefore might coordinate with the central metal ion and can be able to reduce the aggregation. In the UV-Visible spectrum of **TFM-Pc** the characteristic Q-band was observed at 682 nm in DCM. The intense Q-band absorptions were also observed at 680 nm in THF, 685 nm in DMF, 684 nm in Toluene and 685 nm in DMSO. The Q-band absorption in THF is slightly blue shifted compared to other solvents but shows highest molar absorption coefficient, Table 1. Aggregation is usually depicted as coplanar association of phthalocyanine rings which is dependent on concentration, nature of solvent, nature of substituents, central metal ion and temperature. In this study, the aggregation behaviour of **TFM-Pc** was investigated in DCM. The concentration dependence of the absorption spectra of this Pc was assessed to show minimal aggregation. As the concentration was increased to $1.5 \times 10^{-5} \text{ M}$

and above, the absorbance change with concentration started deviating from Beer-Lambert law, Figure 2.

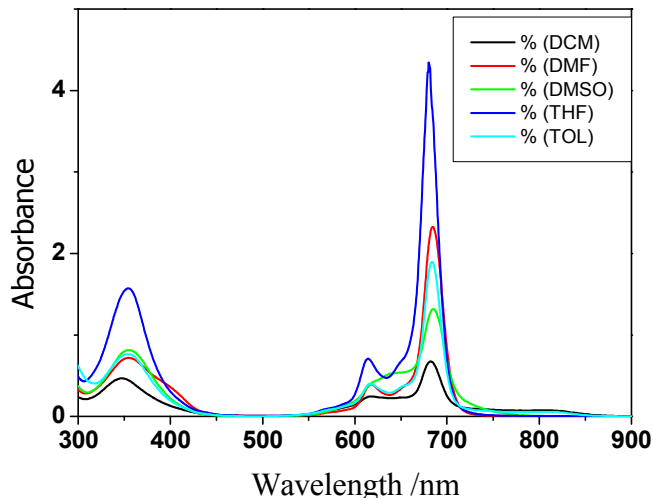


Fig. 1 Absorption spectra of **TFM-Pc** in different solvents at $1.0 \times 10^{-5} \text{ M}$ concentration.

To show that the increase in absorbance values above 700 nm in DCM and toluene is due to J-aggregation, a study of the absorption of the monoprotonated species of **TFM-Pc** was carried to rule out the possibility that this increase in absorbance is not due to the protonated species.⁴³⁻⁴⁶ For protonation, trifluoroacetic acid was added to the **TFM-Pc** solution of DCM. With an increase in the trifluoroacetic acid concentration the absorption at 682 nm was found to decrease and a new band was formed around 700 nm. The Q-band was found to degrade at even higher concentration of acid. Comparison of the absorption spectrum of **TFM-Pc** in DCM at higher concentration and the protonated **TFM-Pc** species spectrum suggests that the absorbance above 700 nm in DCM is not due to the protonation. From Figure 2, it can be said that with an increase in concentration above $1 \times 10^{-5} \text{ M}$ the molar extinction coefficient at 682 nm becomes smaller and the intensity of the band above 700 nm increased. These concentration dependent spectral changes of **TFM-Pc** are typical of J-aggregates.

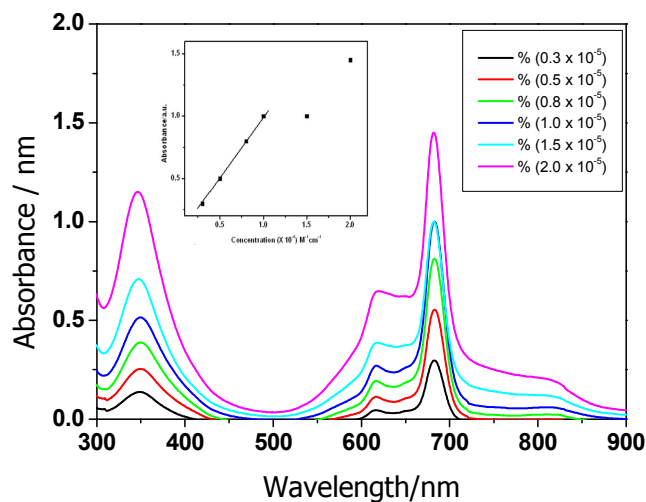


Fig. 2 Absorption spectra of **TFM-Pc** in DCM at different concentrations.

Electrochemical Studies

Phthalocyanine unit is an 18 π -electron aromatic system that, in its common oxidation state, carries two negative charges. This unit is capable of oxidation, by losing one to three electrons, and reduction by gaining one or two electrons. The relative positions of the HOMO and LUMO levels can be shifted via changes in the electron density of the molecule brought about by electron donating or electron withdrawing substituents. To investigate the redox properties of **TFM-Pc**, we have adopted the cyclic voltammetry and differential pulse voltammetry techniques. Figure 3 shows the cyclic voltammogram of **TFM-Pc** in DCM and 0.1 M tetrabutyl ammonium perchlorate (TBAP) using ferrocene is an external standard.

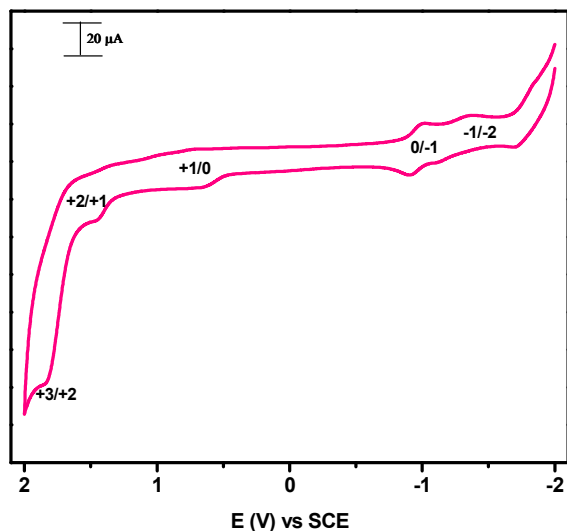


Fig. 3 Cyclic voltammogram of **TFM-Pc** in DCM

Three one electron oxidations and two one electron reductions are observed for this complex when studied in DCM solvent. All the redox processes are of either reversible or quasi-reversible nature. The HOMO-LUMO gap as calculated from the difference between first oxidation and first reduction potential was found to be 1.64 V. The HOMO-LUMO value was found to be within the range that has been noticed previously for other metallophthalocyanines.^{47,48} Based on well-known electrochemical behaviour of phthalocyanine complexes, all couples for **TFM-Pc** are assigned to phthalocyanine ring. The nature of redox couples will also be confirmed using spectro-electrochemical measurements.

Spectroelectrochemical Studies

Spectro-electrochemical studies were performed to monitor changes during redox reactions of the newly synthesized phthalocyanine. Figures 4a-c illustrate the spectral changes of **TFM-Pc** under applied potential. Figure 4a shows the spectra changes during the controlled potential oxidation of **TFM-Pc** at an applied potential of 0.90 V. While the Q-band decreases in intensity, new bands at 510 and 839 nm are recorded during the oxidation process. At the same time the B-band at 349 nm reduces its intensity. The shoulder present at 616 nm which generally represents the aggregation in phthalocyanines was seen to vanish completely during the first oxidation. Clear

isosbestic points were observed at 336, 416, 595 and 714 nm which confirms the generation of new species. These changes are typical of the ring based oxidation and assigned to $[\text{Zn}^{\text{II}}\text{Pc}^{-2}]/[\text{Zn}^{\text{II}}\text{Pc}^{-1}]^{1+}$ process.⁴⁹⁻⁵¹ Spectroscopic changes during the controlled potential application at 1.60 V support the further oxidation of the monocationic species confirming the CV assignment of the couple to $[\text{Zn}^{\text{II}}\text{Pc}^{-1}]^{1+}/[\text{Zn}^{\text{II}}\text{Pc}^0]^{2+}$, as shown in Figure 4b. The band at 510 nm has decreased in intensity. While the Q band further decreased in intensity, the generation of a new band at 738 nm was seen which is known to be characteristic absorption band of Pc cation.

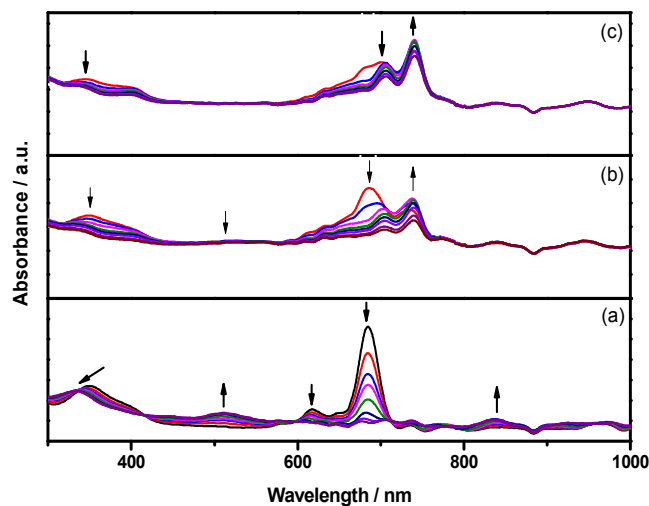


Fig. 4 In-situ UV-Visible absorption changes of **TFM-Pc** at an applied potential of (a) 0.9 V (b) 1.6 V (c) 1.9 V.

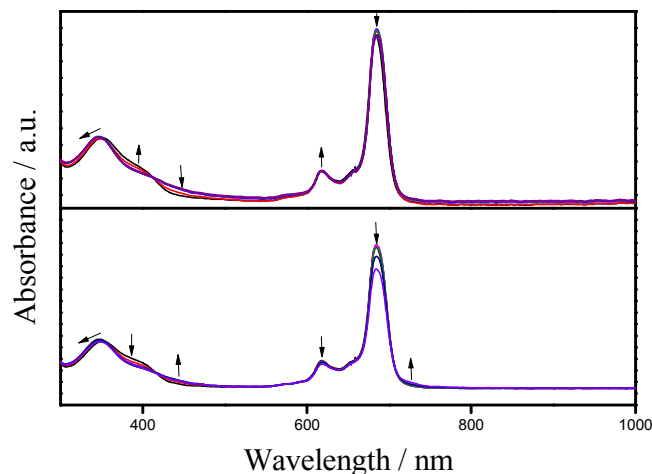


Fig. 5 In-situ UV-Visible absorption changes of **TFM-Pc** at an applied potential of (a) -1.20 V (b) -1.50 V.

Clear isosbestic points were recorded at 416, 555, 588 nm. Almost same changes were observed during third oxidation of the phthalocyanine macrocycle where in the band at 738 nm further increased in intensity while the Q band along with a decrease in the intensity also shifted to 706 nm from 685 nm. These changes in the absorption spectrum were assigned to oxidation of species from $[\text{Zn}^{\text{II}}\text{Pc}]^{+2}$ to $[\text{Zn}^{\text{II}}\text{Pc}]^{+3}$. Fig. 4d shows the spectral changes during reduction process at controlled potential of -1.20 V. The intensity of Q band absorption at 683

nm decreased without shift, while new bands at 404 and 723 nm appeared with increasing intensity. The B band at 348 nm and shoulder at 628 nm decreases in intensity without shift. Clear isosbestic points were recorded at 416 and 707 nm. These changes are typical of the ring based reduction and assigned to $[\text{Zn}^{\text{II}}\text{Pc}^{-2}]/[\text{Zn}^{\text{II}}\text{Pc}^{-3}]^{-1}$ process (Fig. 5).⁴⁹⁻⁵¹ Spectroscopic changes were observed during the controlled potential application at -1.50 V further decreases the intensity of Q-band.

Emission Studies

Qualitative evaluation of emission, including quantitative analysis of the fluorescence spectra and determination of the quantum yields (ϕ_f) was performed for **TFM-Pc** in order to understand the effect of peripheral substitution on phthalocyanine macrocycle. The emission spectra were recorded in different solvents by exciting the phthalocyanine at 680-685 nm. The steady state spectrum of the complex was found to be similar except the different emission maxima when studied in different solvents. Fluorescence quantum yields were determined by the comparative method according to

$$\phi_{\text{sample}} = \frac{F_{\text{sample}} \times \text{Abs}_{\text{standard}}}{F_{\text{standard}} \times \text{Abs}_{\text{sample}}} \times \phi_{\text{standard}}$$

Where ϕ_{sample} is the quantum yield of the sample, ϕ_{standard} is the quantum yield of the standard, F_{sample} is the fluorescence intensity of the sample, F_{standard} is the fluorescence intensity of the standard, $\text{Abs}_{\text{sample}}$ is the absorbance of the sample at excitation wavelength, $\text{Abs}_{\text{standard}}$ is the absorbance of the standard at the excitation wavelength.

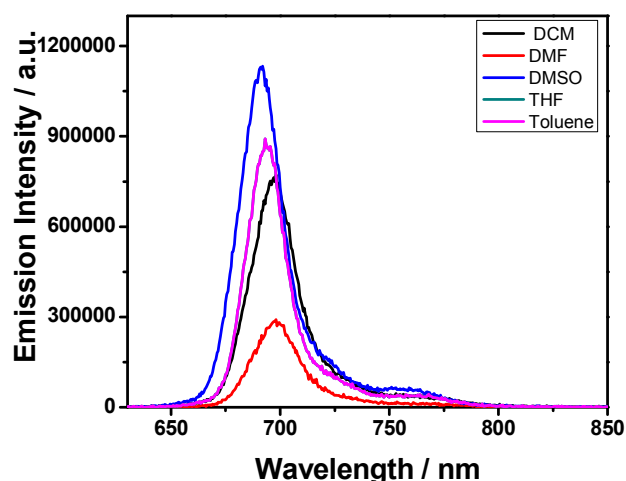


Fig. 6 Steady state fluorescence spectrum of **TFM-Pc** in different solvents.

From the data presented in Fig. 6 it is evident that the emission spectrum of **TFM-Pc** lies within the limits of Stokes rule and the rule of mirror symmetry between the absorption and fluorescence bands. From the data presented in Table 1, it is clear that as the polarity of the solvent increases, the quantum yield is reduced which might be due to the increase of aggregation in polar solvents which reduces the possibility of radiative deactivation i.e., fluorescence through dissipation of

energy by the aggregates and this has direct influence on the excited state life time of the complex. The excited state lifetime decay signal of **TFM-Pc** in different solvents is shown in Fig. 7 and the corresponding data is summarized in Table 1. The complex showed mono-exponential decay in all the solvents studied and a maximum lifetime of 3 ns was found in THF solvent which might tell about the slow degradation of this complex in this solvent following excitation.

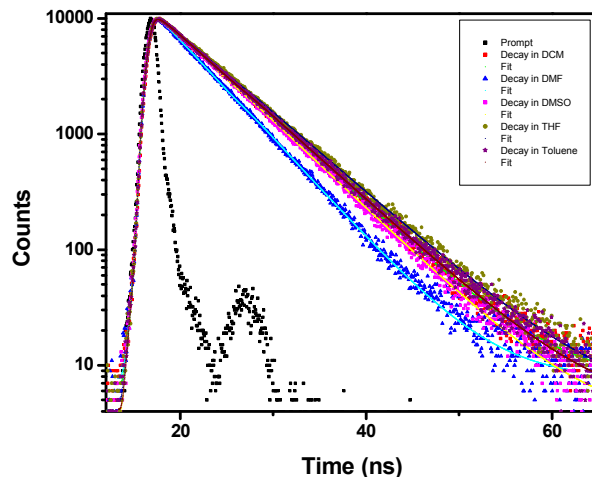


Fig. 7 Excited state lifetime spectra of **TFM-Pc** in different solvents.

Table 1 UV-Visible, emission, excited state life-time data of **TFM-Pc**.

Solvent	λ_{max} , nm ($\log \epsilon$, $\text{M}^{-1}\text{cm}^{-1}$) ^a	λ_{em} , nm	ϕ_f ^b	τ_f (ns)
Toluene	684 (4.83)	693	0.26	2.90
DCM	682 (5.27)	697	0.27	2.83
THF	680 (5.63)	693	0.26	3.02
DMF	684 (5.36)	698	0.09	2.39
DMSO	685 (5.12)	691	0.10	2.76

^aError limits: λ_{max} , ± 1 nm, $\log \epsilon$, $\pm 10\%$. ^bError limits: ϕ_f , $\pm 10\%$.

NLO Results and Discussion

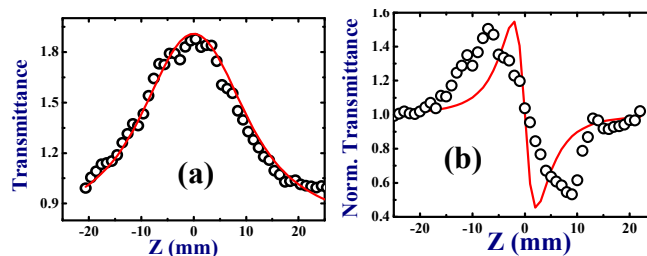


Fig. 8(a) Open aperture and (b) closed aperture data of **TFM-Pc** recorded with ~ 70 fs, 1 kHz pulses at 690 nm.

Figures 8(a) and 8(b) depict the fs open aperture and closed aperture data of **TFM-Pc**, respectively. It is evident that saturable absorption (SA) was the dominant mechanism in open

aperture case. Since the excitation wavelength is 690 nm, where the molecule has strong absorption it is expected to demonstrate SA. The saturation intensity ($I_s = 5.0 \times 10^{11} \text{ W/cm}^2$) was lower than the peak intensity used ($I_{00} = 6.6 \times 10^{11} \text{ W/cm}^2$). The signature of closed aperture data indicates a peak-valley structure suggesting negative nonlinearity. The magnitude of NLO coefficient n_2 was $6.8 \times 10^{-17} \text{ cm}^2/\text{W}$. Since the pulses are too short ($<100 \text{ fs}$ duration with true 1 kHz repetition rate) the value of NLO coefficient clearly represents the pure electronic contribution.

Figures 9(a) and 9(b) depict the ps open aperture and closed aperture data of TFM-Pc, respectively. Open aperture data clearly suggests the presence of reverse saturable absorption (RSA) type of behaviour recorded at a peak intensity of 82 GW/cm^2 . In this case we fitted the data for an effective two-photon absorption (2PA) coefficient. There is a possibility of excited state absorption contribution to the observed RSA. Further detailed intensity dependent studies are required to decouple the contribution of excited state absorption in the present case. The value of 2PA (β_{eff}) coefficient obtained from the fit to experimental data was $5.9 \times 10^{-12} \text{ cm/W}$. The closed aperture data again suggested negative nonlinearity with a magnitude of $1.64 \times 10^{-15} \text{ cm}^2/\text{W}$. The huge magnitude of n_2 obtained in this case when compared to the fs case indicates the contribution of other processes to the overall optical nonlinearity apart from purely electronic contribution. The large n_2 value obtained in the ps case clearly suggests the possible involvement of excited state population to the overall nonlinearity. The NLO coefficients obtained for this molecule are on par with some of the recently reported molecules from our group.^{15,16,22,33}

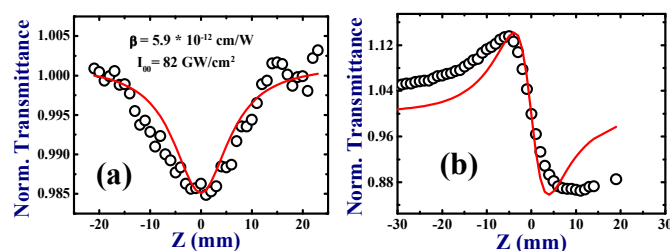


Fig. 9 (a) Open aperture and (b) closed aperture data of TFM-Pc recorded with $\sim 2 \text{ ps}$, 1 kHz pulses at 800 nm .

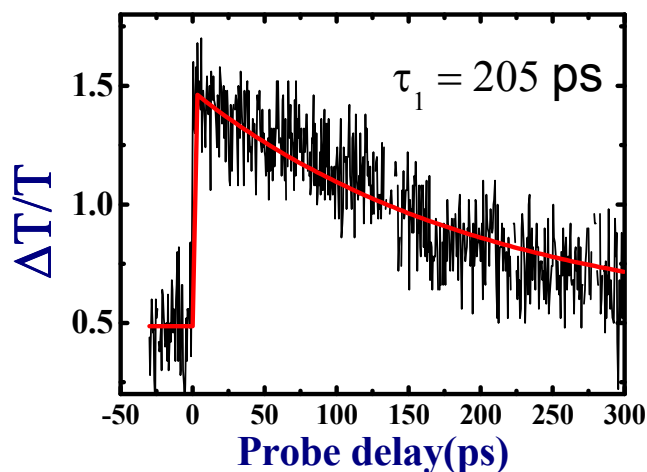


Fig. 10 Degenerate pump-probe data of TFM-Pc recorded with $\sim 70 \text{ fs}$ pulses at a wavelength of 690 nm .

Figure 10 depicts the fs pump-probe data obtained for TFM-Pc at 690 nm . The data clearly directs to bleaching of ground state population. The data was fitted to a single exponential decay constant of $\sim 205 \text{ ps}$. The radiative lifetime in this compound is in the ns regime as confirmed from the radiative lifetime measurements. The decay constant obtained indicates the presence of non-radiative decay processes (through release of energy to the solvent) from the first excited singlet state to ground state and/or triplet states. Our future studies will focus on doping this molecule in a suitable polymer and evaluate the enhanced NLO coefficients and explore the possible applications in the field of optical limiting and all-optical switching.

Conclusions

A novel Zinc phthalocyanine has been synthesized and its optical, emission, electrochemical and third-order NLO properties were investigated. Electrochemical properties indicated that both oxidation and reduction processes were ring centred. The emission spectra were recorded in different solvents and the fluorescence yields obtained were in the range of 0.29 to 0.10 . The time-resolved fluorescence data revealed lifetimes of typically few ns. Z-scan measurements using ps and fs pulses revealed strong NLO coefficients suggesting the potential of this molecule for applications in photonics. Excited state lifetime of $\sim 205 \text{ ps}$ was deduced from the fs degenerate pump-probe measurements and attributed to the non-radiative decay from first excited state.

Acknowledgements

L.G. thanks CSIR-XII FYP 'Intel Coat' project CSC-0114. V.K.S. and N.V.K. thank CSIR for research fellowships. S.V.R. and D.S. thank DRDO for continued financial support.

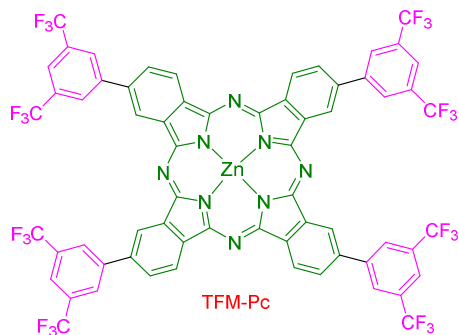
References

1. D. Wöhrle, G. Schnurpfeil, S.G. Makarov, A. Kazarin, O.N. Suvorova, *Macromolecules*, 2012, **45**, 191.
2. T. Nyokong, *Pure Appl. Chem.* 2011, **83**, 1763.
3. G. de la Torre, P. Vazquez, F. Agullo-Lopez, T. Torres, *Chem. Rev.*, 2004, **104**, 3723.
4. A. Colombo, F. Nisic, C. Dragonetti, D. Marinotto, I.P. Oliveri, S. Righetto, M.G. Lobello, F. De Angelis, *Chem. Commun.*, 2014, **50**, 7986.
5. S. Suresh, A. Ramanand, D. Jayaraman, P. Mani, *Rev. Adv. Mater. Sci.* 2012, **30**, 175.
6. E.D. D'silva, G.K. Podigatipalli, S. Venugopal Rao, S.M. Dharmaprasanth, *Optics & Laser Technology*, 2012, **44**, 1689.
7. H. Liu, C. Chen, F. Xi, P. Wang, S. Zhang, P. Wu, C. Ye, *J. Nonlinear Optic. Phys. Mat.*, 2001, **10**, 423.
8. N. Venkatram, L. Giribabu, D. Narayana Rao, S. Venugopal Rao, *Appl. Phys. B* 2008, **91**, 149.
9. W. Sun, G. Wang, Y. Li, M.J.F. Calvete, D. Dini, M. Hanack, *J. Phys. Chem. A*, 2007, **111**, 3263-3270.
10. M. Hanack, D. Dini, M. Barthel, S. Vagin, *The Chem. Record*, 2002, **2**, 129.
11. Y. Chen, S. O'Flaherty, M. Fujitsuka, M. Hanack, L.R. Subramanian, O. Ito, W.J. Blau, *Chem. Mater.* 2002, **14**, 5163.
12. N. Venkatram, L. Giribabu, D. Narayana Rao, S. Venugopal Rao, *Chem. Phys. Lett.*, 2008, **464**, 211.

13. S.J. Mathews, S. Chaitanya Kumar, L. Giribabu, S. Venugopal Rao, *Opt. Commun.*, 2007, **280**, 206.
14. G.S. He, G.C. Xu, P.N. Prasad, B.A. Reinhardt, J.C. Bhatt, A.G. Dillard, *Opt. Lett.*, 1995, **20**, 435.
15. D. Swain, A. Rana, P.K. Panda, S. Venugopal Rao, *Chem. Phys. Lett.*, 2014, **610-611**, 310.
16. D. Swain, T. Sarma, P.K. Panda, S. Venugopal Rao, *Chem. Phys. Lett.*, 2013, **580**, 73.
17. R.K. Choubey, S. Medhekar, R. Kumar, S. Mukherjee, S. Kumar, *J Mater Sci. Mater. Electron.*, 2014, DOI 10.1007/s10854-014-1743-3.
18. S. Venugopal Rao, *Proc. SPIE*, 2010, **7728**, 77281N
19. "Phthalocyanines Properties and Applications," Ed.'s C. C. Leznoff, A. B. P. Lever, 1993, Wiley VCH publishers, New York.
20. S.J. Mathews, S. Chaitanya Kumar, L. Giribabu, S. Venugopal Rao, *Mater. Lett.*, 2007, **61**, 4426.
21. D. Swain, V.K. Singh, N.V. Krishna, L. Giribabu, S. Venugopal Rao, *J. Porphyrins & Phthalocyanines*, 2014, **18**, 305.
22. S. Hamad, Surya P. Tewari, L. Giribabu, S. Venugopal Rao, *J. Porphyrins & Phthalocyanines*, 2012, **16**, 140.
23. F. Dumoulin, M. Durmuş, V. Ahsen, T. Nyokong. *Coord. Chem. Rev.*, 2010, **254**, 2792.
24. H. Bertagnolli, W.J. Blau, Y. Chen, D. Dini, M.P. Feth, S.M. O'Flaherty, M. Hanack, V. Krishnan, *J. Mater. Chem.*, 2005, **15**, 683.
25. A. Santhi, V.V. Naboodiri, P. Radhakrishnan, V.P.N. Nampoori, *J. Appl. Phys.*, 2006, **100**, 053109.
26. K.P. Unnikrishnan, J. Thomas, V.P.N. Nampoori, C.P.G. Vallabhan, *Appl. Phys. B*, 2002, **75**, 871.
27. F.Z. Henari, *J. Opt. A.: Pure Appl. Opt.*, 2001, **3**, 188.
28. G. Torre, P. Vazquez, F. Aquillo-Lopez, T. Torres. *J. Mater. Chem.* 1998, **8**, 1671.
29. A.B. Sorokin. *Chem. Rev.* 2013, **113**, 8152.
30. M.E. Ragoussi, M. Ince, T. Torres. *Euro J. Org. Chem.* 2013, 6475.
31. V.K. Singh, R.K. Kanaparthi, L. Giribabu, *RSC Adv.* 2014, **4**, 6970.
32. K. Ishii, N. Kobayashi, K.M. Kadish, K.M. Smith and R. Guilard, *The Porphyrin Handbook*, Vol.16, Academic Press/Elsevier, New York, 2003; (Chapter 102):1-40.
33. D. Swain, V.K. Singh, N.V. Krishna, L. Giribabu, S. Venugopal Rao, *J. Mater. Chem. C*, 2014, **2**, 1711.
34. N. Lida, E. Tokunga, N. Saito, N. Shibata, *J. Fluorine Chem.* 2014, **168**, 93.
35. S. Vagin, M. Hanack, *Eur. J. Org. Chem.*, 2004, 600.
36. L. Gao, X. Qian, L. Zhang, Y. Zhang, *J. Photochem. Photobiol. B. Biol.*, 2001, **65**, 35.
37. D. S. Lawrence, D. G. Whitten, *Photochem. Photobiol.*, 1996, **64**, 923.
38. P.T. Anusha, P.S. Reeta, L. Giribabu, S.P. Tewari, S. Venugopal Rao, *Mater. Lett.*, 2010, **6**, 1915.
39. K.V. Saravanan, K.C. James Raju, M.G. Krishna, S.P. Tewari, S. Venugopal Rao, *Appl. Phys. Lett.*, 2010, **96**, 232905.
40. G.K. Podagatlapalli, S. Hamad, S. Sreedhar, S.P. Tewari, S. Venugopal Rao, *Chem. Phys. Lett.*, 2012, **530**, 93.
41. S. Venugopal Rao, *J. Mod. Opt.*, 2011, **58**, 1024.
42. A. Ceulemans, W. Oldenhof, C. Gorrler-Walrand, L.G. Vanquickenborne, *J. Am. Chem. Soc.*, 1986, **108**, 1155.
43. G. Bottari, A. Kahnt, D.M. Guldi, T. Torres, *J. Solid State Sci. & Technology*, 2013, **2**, M3145.
44. K. Palewska, J. Sworakowski, J. Lipinski, *Opt. Mater.*, 2012, **34**, 1717.
45. E. Onal, F. Dumoulin, C. Hirel, *J. Porphyrins & Phthalocyanines*, 2009, **13**, 702.
46. L. Jianbo, Z. Yu, Z. Fuqun, Z. Fushi, T. Yingwu, S. Xinqi, C. Foo-Tiem, *Acta Physico Chimica Sinica*, 1996, **12**, 202.
47. K. Sakamoto, E. Ohno-Okumura, *Materials*, 2009, **2**, 1127.
48. K.M. Kadish, G. Moninot, Y. Hu, D. Dubois, A. Ibnlfassi, J.-M. Barbe, R. Guilard, *J. Am. Chem. Soc.*, 1993, **115**, 8513.
49. B. Simicglavaski, S. Zecevic, E. Yeager. *J Electrochem Soc.*, 1987, **134**, C130.
50. B. Agboola, K. I. Ozoemena, T. Nyokong. *Electrochim Acta*, 2006, **51**, 4379.
51. Z. Ou, Z. Jiang, N. Chen, J. Huang, J. Shen, K. M. Kadish, *J. Porphy. Phth.*, 2008, **12**, 1123.

Optical, electrochemical, third order nonlinear optical, and excited state dynamics studies of *bis*(3,5-trifluoromethyl)phenyl-zinc phthalocyanine

Narra Vamsi Krishna, Varun Kumar Singh, Debasis Swain, Soma Venugopal Rao, Lingamallu Giribabu



Zinc phthalocyanine substituted with *bis*(3,5-trifluoromethyl)phenyl groups at peripheral positions have been synthesised and characterised using absorption, fluorescence and electrochemical techniques. The new phthalocyanine obey Beer-Lambert Law upto milli molar concentration. Spectroelectrochemical properties indicate that the redox reactions are belongs to macrocyclic center. Finally, the excited state dynamics in this molecule have been investigated using fs degenerate pump-probe spectroscopy.